Electroluminescence of Multicomponent Conjugated Polymers. 1. Roles of Polymer/Polymer Interfaces in Emission Enhancement and Voltage-Tunable Multicolor Emission in Semiconducting Polymer/Polymer Heterojunctions

Xuejun Zhang and Samson A. Jenekhe*

Department of Chemical Engineering and Center for Photoinduced Charge Transfer, University of Rochester, Rochester, New York 14627-0166

Received November 12, 1999; Revised Manuscript Received January 19, 2000

ABSTRACT: Effects of the electronic structure of polymer/polymer interfaces on the electroluminescence efficiency and tunable multicolor emission of polymer heterojunction light-emitting diodes were explored by a series of 16 n-type conjugated polymers with varying electron affinities and ionization potentials in conjunction with poly(*p*-phenylenevinylene). Efficiency and luminance of diodes of the type indium−tin oxide/poly(*p*-phenylenevinylene)/n-type polymer/aluminum were maximized and were as high as 3% photons/electron and 820 cd/m^2, respectively, when the energetics at the polymer/polymer interface favored electron transfer while disfavoring hole transfer. Energetic barrier to electron transfer at the polymer/polymer interface was more important to electroluminescence efficiency and diode luminance than injection barrier at the cathode/polymer interface. By a judicious choice of the relative layer thicknesses and the components of the bilayer heterojunctions, the rate of both electron and hole transfer across the polymer/polymer interface can be regulated by the applied voltage, resulting in continuous voltage tunability of emission colors. The voltage tunable multicolor emission is exemplified by red (5 V) ↔ yellow (9 V) ↔ green (12 V) and other intermediate color switching in poly(*p*-phenylenevinylene)/poly(2,6-(4-phenyl)-quinoline) (PPQ) diodes. The multicolors obtained from a single heterojunction diode by varying the applied voltage originated from the mixing of the component emission spectra in varying proportions facilitated by interfacial charge transfer and finite size effects. Electroluminescence microscopy was used to directly image the multicolor diodes. These results suggest that the electronic structure of polymer/polymer interfaces and finite size effects dominate the emission features and performance of light-emitting devices based on multicomponent polymers such as multilayered thin films, phase-separated blends, and block copolymers. The results also have implications for photovoltaic cells and other optoelectronic devices using conjugated polymers.

Introduction

Conjugated polymers in their native state are molecular semiconductors which are of growing interest in optoelectronic and electronic devices, including light-emitting diodes (LEDs),[1,2] lasers,[3] photovoltaic cells,[4] xerographic imaging photoreceptors,[5] and thin-film transistors.[6] In the case of polymer LEDs, synthetic manipulation of macromolecular architecture has made available diverse light-emitting conjugated polymers from which LEDs of various colors have been fabricated and are now being optimized by a variety of device engineering strategies. In efforts to design next generation electroluminescent (EL) materials with significantly improved EL efficiency and to explore novel phenomena (for example, multicolor emission,[7,8] exciplex emission,[9] and photon harvesting/energy transfer[10]) not feasible in conjugated homopolymers, multicomponent conjugated polymer systems, which include multilayered thin films,[8,11,12] blends,[7,10,13,14] and block copolymers,[15] are of increasing interest. The present study focuses on the electronic structure and properties of polymer/polymer interfaces in view of their expected roles in the photophysics and charge-transfer processes in multicomponent conjugated polymers and devices made from them.

In the simplest polymer LED, an EL polymer thin film, such as poly(*p*-phenylenevinylene) (PPV), is sandwiched between two electrodes of different work functions as schematically shown in Figure 1a. Such a single-layer polymer LED is generally inefficient for two principal reasons. First, there is poor charge injection at one or both metal/polymer interfaces due to the inability to simultaneously match the anode work function (Φ_a) to the highest occupied molecular orbital (HOMO) and the cathode work function (Φ_c) to the lowest unoccupied molecular orbital (LUMO) of the polymer. The energy barriers to hole and electron injection at the anode and cathode are respectively ΔE_h ($= \Phi_a - IP$) and ΔE_e ($= \Phi_c - EA$) where IP is the ionization potential and EA is the electron affinity of the polymer (Figure 1a). Second, there is a huge disparity between hole and electron mobilities in semiconducting polymers,[16] thus precluding balanced charge transport in the devices. Commonly studied EL polymers such as PPV,[1a] polyphenylenes,[17] polyfluorenes,[18] polythiophenes,[7] and their derivatives are p-type (hole transport) polymers which have hole mobilities that are orders of magnitude larger than electron mobilities, relatively small barriers to hole injection from indium−tin oxide (ITO, $\Phi_a \sim 4.7-4.8$ eV),[19a] and very large barriers to electron injection from air-stable cathodes such as aluminum ($\Phi_c \sim 4.0-4.3$ eV).[19b] Two-layer polymer/polymer heterojunction LEDs, schematically shown in Figure 1b, have been found to have dramatically improved EL efficiency and brightness,[8a,8b,12] compared to the one-layer devices (Figure 1a), as also found in multilayered organic/organic diodes.[20]

n-Type (electron transport) polymers used in such two-layer heterojunction LEDs are thought to improve

10.1021/ma991913k CCC: $19.00
Published on Web 02/25/2000

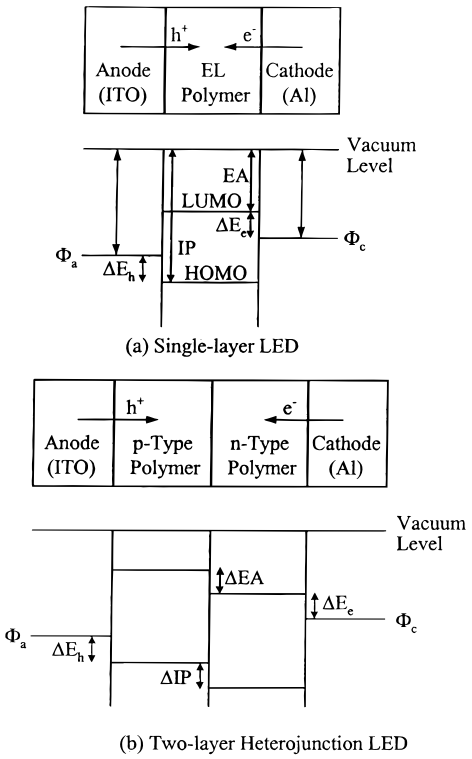

Figure 1. Schematic illustration of (a) a single-layer polymer LED and (b) a two-layer heterojunction LED and their associated energy levels.

Chart 1

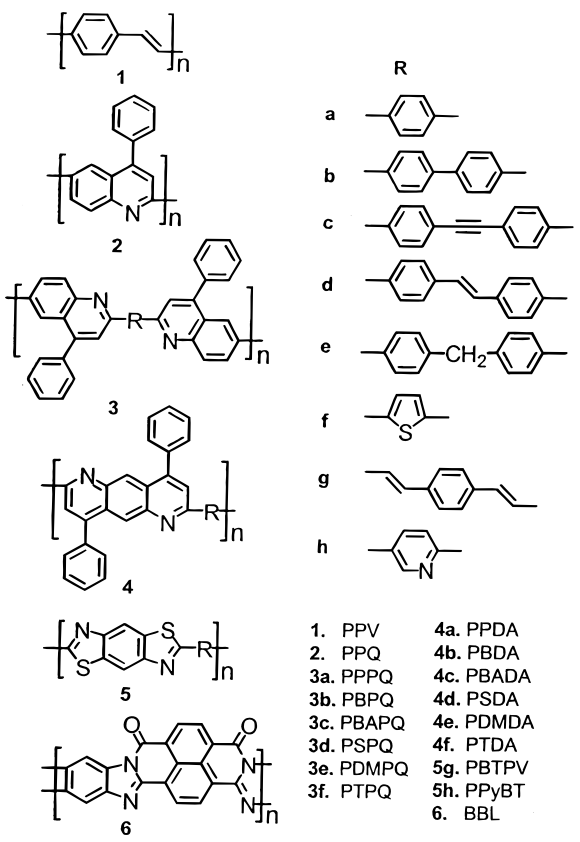

device efficiency through their high electron affinities which reduce the barrier to electron injection at the cathode/polymer interface.[12c] An increasing part of current EL materials research effort is thus being directed to the design and synthesis of n-type polymers with improved properties.[12] Both nonconjugated polymers, such as the oxadiazole-containing side-chain polymers,[12a,b] and π-conjugated polymers, such as poly(cyanoterephthalylidene)s (CN-PPVs),[12c] poly(phenylquinoxaline)s,[12d–f] polypyridines,[12g] and polyquinolines,[8a] have been reported as electron transport layers in two-layer heterojunction LEDs. What is currently lacking, however, is the understanding of the roles of the electronic structures and sizes of the polymer/polymer interfaces in such two-layer heterojunction LEDs. In contrast, extensive studies of metal/polymer interfaces[21] in LEDs have provided knowledge of their general features and properties in relation to device performance. For example, the ITO/PPV interface is believed to be quasi-ohmic, if not ohmic, for hole injection,[22a] whereas the cathode (Al, Ca, Mg)/PPV interface injects electrons by tunneling and/or other complex processes.[22b] The Al/PPV interface is known to exhibit Schottky barrier characteristics, leading to photovoltaic properties.[4a]

In addition to their possible important roles in the two-layer heterojunction LEDs (Figure 1b), polymer/polymer interfaces can also play a critical role in even single-layer LEDs (Figure 1a) if the polymer layer consists of a phase-separated blend[7] or a microphase-separated block copolymer. More generally, polymer/polymer interfaces mediate a variety of photophysical and charge-transfer processes in multicomponent conjugated polymer systems exemplified by efficient energy transfer in binary nanophase-separated blends[10] and block copolymers,[15a] exciplex formation[9] in bilayers and blends, ground-state electron transfer in binary blends,[13a] photoinduced electron transfer in binary blends,[13b] and tunable multicolor electroluminescence in bilayers[8] and blends.[7] The coupling of *finite size effects* to the electronic structure and properties of polymer/polymer interfaces in such multicomponent polymers has been suggested from observed multicolor EL emission from two-layer heterojunctions.[8a] Conjugated polymer bilayer heterojunctions have also been extensively studied as rectifying junctions (charge trapping electrodes, charge storage) in electrochemical experiments.[23]

In this paper we report on studies focusing on the two-layer polymer heterojunction LED structure of Figure 1b and addressing the question of what influence the electronic structure of the polymer/polymer interface has on the EL diode efficiency and luminance. Finite size effects on the polymer/polymer bilayer heterojunctions were also explored. We view this planar heterojunction as an ideal model system for investigating the electronic structure and properties of polymer/polymer interfaces; well-defined planar heterojunctions of diverse conjugated polymers and layer thicknesses can be prepared by a number of polymer processing techniques. We used PPV on ITO as the model p-type EL polymer. A total of 16 conjugated polymers, which are known to exhibit reversible electrochemical reduction[24] and other n-type (electron transport) characteristics,[5,25] provided a range of electron affinities and ionization potentials that allowed the electronic structure of PPV/n-type polymer interface to be varied and probed. These n-type semiconducting polymers whose molecular structures are shown in Chart 1 include seven polyquinolines (PQs),[24a,26a] six polyanthrazolines (PATs),[24a,26a,b] two polybenzobisthiazoles (PBTs),[24b,c,26c] and one poly(benzimidazobenzophenanthroline ladder) (BBL).[13,24c] The layer thicknesses of PPV and the n-type polymer in a bilayer heterojunction were varied to probe size effects and multicolor EL emission. In addition to spectroscopic

and electrical measurements, we also used electroluminescence microscopy to characterize the heterojunction LEDs.

Experimental Section

Materials. The molecular structures of PPV and all the n-type semiconducting polymers used in this study are shown in Chart 1. The sulfonium precursor of PPV (**1**) in ~1 wt % methanol solution was purchased from Lark Enterprises (Webster, MA). Polyquinolines (**2**, **3a**−**3f**),[24a,26a] polyanthrazolines (**4a**−**4f**),[24a,26a,b] polybenzobisthiazoles (**5g**, **5h**),[24b,c,26c] and BBL (**6**)[24c] were synthesized in our laboratory. Their syntheses and characterizations have been previously reported.[24,26]

Fabrication of Polymer/Polymer Heterojunction LEDs. Figure 1b shows the schematic structure of the semiconducting polymer heterojunction LEDs. In the heterojunction devices, indium−tin oxide (ITO) was used as the anode, PPV (25−130 nm) was used as the p-type layer, the various n-type conjugated polymers (15−100 nm) shown in Chart 1 were each used as an n-type layer, and aluminum (Al) was used as the cathode. ITO-coated glass substrates (Donelly Corp., Holland, MI) were cleaned sequentially in ultrasonic bathes of detergent, 2-propanol/deionized water (1:1 volume) mixture, toluene, deionized water, and acetone. PPV thin films (25−130 nm) were deposited onto the ITO-coated glass substrates by spin-coating of the sulfonium precursor from methanol solutions followed by thermal conversion in a vacuum (220−250 °C for 1−2 h). For PPV single-layer devices, the PPV film thickness was 70 nm. Thin films of polyquinolines (PQs) and polyanthrazoline (PATs) were spin-coated from their formic acid solutions onto the vacuum-dried (converted) PPV layer and then dried in a vacuum at 60 °C for 12 h to remove the solvent (formic acid). Thin films of polybenzobisthiazoles (PBTs) and BBL were spin-coated onto the PPV layer from their reversibly soluble Lewis acid ($GaCl_3$) coordination complexes in nitromethane.[27] All solutions were filtered with a 0.2 μm (pore size) Acrodisc 13 CR PTFE syringe filter (Pall Corp., East Hills, NY) before spin-coating. The film thicknesses were measured by an Alpha-step profilometer (model 200, Tencor Northern, San Jose, CA) with an accuracy of ±1 nm and confirmed by an optical absorption coefficient technique. The film thickness was controlled by adjusting the spin-coating speed (1000−3000 rpm) and polymer solution concentrations (0.1−1 wt %). Finally, 100−130 nm aluminum electrodes were vacuum ($<5 \times 10^{-6}$ Torr) evaporated onto the resulting polymer bilayers. The area of each device was about 0.2 cm^2 (5 mm diameter), and there were nine devices per substrate.

Characterization of Polymer Heterojunction LEDs. Electroluminescence (EL) spectra were obtained by using a Spex Fluorolog-2 spectrofluorimeter. Current−voltage characteristics of LEDs were measured by using an HP4155A semiconductor parameter analyzer (Yokogawa- Hewlett-Packard, Tokyo). The luminance (brightness) was measured by using a Grasby S370 optometer (Grasby Optronics, Orlando, FL) equipped with a calibrated luminance sensor head (model 211). The model 211 sensor head can accurately measure the luminance of LEDs of spot size as small as 0.8 mm diameter when assembled together with a model 1220 reflex viewing module with 5× microscope objective lens. The current−voltage and luminance−voltage curves were recorded simultaneously by hooking up the semiconductor parameter analyzer together with the optometer.

The quantum efficiencies of the diodes were measured by using procedures similar to those previously reported.[28] Photons emitted from LEDs were detected with a calibrated Grasby 221 photodiode (350−1100 nm, built into a Grasby 2550 integrating sphere). Quantum efficiencies reported in this paper refer to internal efficiencies assuming a refractive index of 1.6 for the semiconducting polymers used to fabricate EL devices.[29] Additional detailed procedures of measuring EL efficiencies of polymer LEDs have been reported elsewhere.[30a] Electroluminescence microscopy of the heterojunction LEDs was done by using an Olympus model BX60 fluorescence/optical microscope (Olympus America, Melville, NY) with an attached digital camera which imaged the true colors of light emitted from the LEDs. The electric-field-modulated photoluminescence (PL) spectroscopy on EL devices was performed the same way as normal PL measurement[30b] except that an electric field was applied to the EL device. The detailed procedure of the electric field-modulated PL spectroscopy was given elsewhere.[14b,15b] All the device fabrication and measurements were performed under ambient laboratory conditions.

Characterization of Photophysical Properties of Bilayer Polymer Heterojunction Thin Films. Representative bilayer polymer/polymer heterojunction thin films such as PPQ/PPV, PPPQ/PPV, PBTPV/PPV, and BBL/PPV were also probed by the optical absorption spectroscopy, steady-state PL spectroscopy, and picosecond time-resolved PL decay dynamics in order to understand better any photophysical processes occurring at the polymer/polymer interfaces. For these measurements, the bilayer heterojunction thin films were prepared in the same way as for the LEDs except that the substrates were silica instead of ITO-coated glass. Typically, the PPV layer was 10−30 nm thick and the n-type layer was 15−30 nm thick.

Optical absorption spectra were obtained by using a Perkin-Elmer Lambda 9 spectrophotometer. PL spectra were obtained by using a Spex Fluorolog-2 spectrofluorimeter. The films for steady-state PL studies were positioned such that the light emission was detected at 22.5° from the incident beam. PL spectra of single-layer thin films (such as PPV) were corrected for the optical density (OD) of the film at the excitation wavelength (λ_{ex}) by a factor of $(1 - 10^{-OD(\lambda_{ex},PPV)})$, where OD($\lambda_{ex}$,PPV) is the optical density of PPV thin film at the excitation wavelength (λ_{ex}). PL intensities of PPV in the bilayers such as PPV/BBL were additionally corrected for the absorption of the excitation light (λ_{ex}) and the reabsorption of the emission light (λ_{em}) by the n-type layer (such as BBL) by factors of $10^{-OD(\lambda_{ex},BBL)}$ and $10^{-OD(\lambda_{em},BBL)}$, respectively, where OD(λ_{ex},BBL) and OD(λ_{em},BBL) are optical densities of the BBL layer at the excitation wavelength (λ_{ex}) and the emission wavelength (λ_{em}), respectively. Time-resolved photoluminescence decay measurements were performed by using the time-correlated single-photon counting technique.[5c,30b] The excitation system consists of a cavity pumped dye laser (Coherent model 703D) circulating rhodamine 6G, synchronously pumped by a mode-locked frequency-doubled Nd:YAG laser (Quantronics model 416). The dye laser pulses were typically 10 ps duration at a repetition rate of 38 MHz, and the samples were excited at 420 nm. The PL decay was detected around the PL emission peak of PPV (540 nm).

Results and Discussion

A. Structure and Properties of Semiconducting Polymer/Polymer Interfaces. Very little is currently known about the *supramolecular structure* or local morphology, electronic structure, and electronic properties of the interfaces between conjugated polymer thin films. In contrast, there is an extensive literature on the chemical structure, composition, size, and mechanical properties of the interfaces between conventional flexible-coil polymers such as polystyrene/polyisoprene and polystyrene/poly(methyl methacrylate).[31] Because of the extensive interdiffusion between such flexible-coil polymers at an interface, the size of the interface region can range from 5 to 100 nm.[31] However, on the ground of their stiff rodlike conformations, we propose that the interfaces between π-conjugated polymers, such as prepared by sequential spin-coating in the present study, can be assumed to be relatively sharp as shown by the schematic illustration of Figure 2. The lack of solubility or swelling of PPV in the solvents from which the n-type conjugated polymers were spin-coated is an important factor in achieving the bilayer heterojunctions with sharp interfaces. The fact that rodlike polymers have much larger relaxation times or smaller diffusion

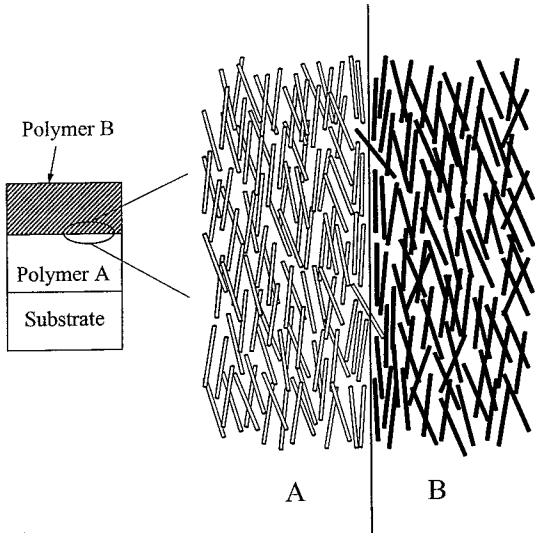

Figure 2. Schematic model of the interface between sequentially spin-coated amorphous thin films of two conjugated polymers A and B which are assumed to be rodlike chains.

constants, compared to flexible coil polymers, is an additional factor favoring relatively sharp interfaces.[31] Because chains of a rodlike polymer at or near an interface can generally have only translational and rotational Brownian motions, they tend to be confined to their side of the interface.[31] The macroscopic morphology (planarity) of the conjugated polymer/conjugated polymer interfaces will, of course, depend on the roughness or smoothness of the first polymer (PPV) layer deposited. Highly planar interfaces can be expected because the spin-coating of Newtonian or non-Newtonian polymer solutions does lead to quite planar surfaces of deposited polymer thin films regardless of any nonuniformity in the substrate.[32] Despite the expected sharpness of the PPV/n-type polymer interfaces, good adhesion between the sequentially deposited layers was observed. We explain this as due to strong van der Waals and $\pi-\pi$ interactions across the interface between the essentially rodlike π-conjugated polymers.

The energy level diagram shown in Figure 1b in terms of the HOMO/IP and LUMO/EA of the two polymers in a bilayer heterojunction assumes flat bands which are commonly observed in organic/organic interfaces.[33] To characterize the electronic structure of the polymer/polymer heterojunctions, we used the HOMO/IP and LUMO/EA values established from the electrochemical redox properties of the pure polymer thin films which were referenced against the saturated calomel electrode (SCE).[24,34a] Both the vacuum level and the SCE energy level relative to it can be difficult quantities to measure precisely in organic semiconductors and conjugated polymers.[33,34b,c] An SCE energy level of 4.4 eV below vacuum[34b] was used as the reference for establishing the IP and EA values of these polymers[13a,24] which are collected in Table 1. The series of n-type polymers have electron affinities in the range 2.36−4.0 eV compared to 2.71 eV for PPV. Similarly, their ionization potentials in the range 5.06−5.90 eV vary widely compared to PPV (5.11 eV). The electronic structure of the series of PPV/n-type polymer bilayer heterojunctions can thus be expected to vary widely and provide insights into the effects of such polymer/polymer interfaces on the performance of LEDs and other optoelectronic devices.

A schematic of the HOMO/IP and LUMO/EA levels of all the n-type semiconducting polymers and those of PPV is shown in Figure 3. On the basis of these zero-field energy levels, one sees that all the PPV/polyquinoline (PQ) and PPV/polybenzobisthiazole (PBT) heterojunctions have interfacial energetics that favor electron transfer from the n-type polymer layer while there is barrier to hole transfer from the PPV layer. Bilayer heterojunctions of the PPV/polyanthrazoline (PAT) type have energetic barriers to both electron and hole transfer except in PPV/PTDA where hole transfer from PPV is feasible. The interface electronic structure of PPV/BBL shows very large barriers to both electron and hole transfer across the interface. For later use in quantitative comparison of the effects of the interface electronic structure on electroluminescence, we define these barriers to hole and electron transfer as ΔIP = IP(n-type polymer) − IP(PPV) and ΔEA = EA(n-type polymer) − EA(PPV), respectively. In the presence of high electric fields additional considerations may enter into the picture of charge transfer across the polymer/polymer interface due to possible electric field-induced charge-transfer processes.

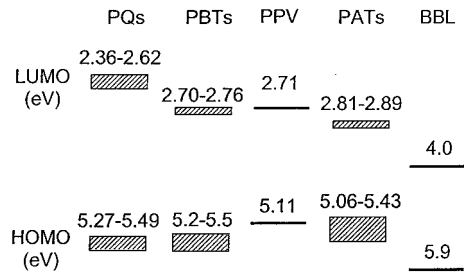

Figure 3. Schematic HOMO/IP and LUMO/EA levels of PPV and all the n-type polymers studied.

Table 1. Electronic Structure Parameters and Photophysical Properties of Conjugated Polymer Thin Films

polymer	EA, eV	IP, eV	λ_{max}^{ABS}, nm	E_g^{opt}, nm	λ_{max}^{PL}, nm
1, PPV	2.71	5.11	408	515	528, 559
2, PPQ	2.62	5.35	414	468	578
3a, PPPQ	2.50	5.47	400	446	574
3b, PBPQ	2.42	5.49	405	441	571
3c, PBAPQ	2.47	5.48	407	456	564
3d, PSPQ	2.48	5.35	414	468	590
3e, PDMPQ	2.36	5.44	380	412	542
3f, PTPQ	2.56	5.27	471	498	622
4a, PPDA	2.83	5.27	443	505	618
4b, PBDA	2.86	5.34	415	485	600
4c, PBADA	2.89	5.36	428	482	628
4d, PSDA	2.81	5.27	451	504	644
4e, PDMDA	2.85	5.43	405	460	590
4f, PTDA	2.87	5.06	500	571	706
5g, PBTPV	2.70	5.20	475, 508	590	630
5h, PPyBT	2.76	5.60	440, 470	500	560
6, BBL	4.00	5.90	568	680	720

The possible occurrence of photophysical processes at the polymer/polymer interfaces in these bilayer heterojunctions may also be anticipated from the HOMO/LUMO energy levels of Figure 3. For example, exciton energy transfer seems feasible in the PPV/polyquinoline heterojunctions. However, except in one case (PPV/PBTPV) where there is some overlap between the absorption spectrum of PBTPV (**5g**) and the emission spectrum of PPV, the necessary absorption/emission overlap for efficient exciton energy transfer[10a] was nonexistent in all the bilayer heterojunctions. Exciplex formation[5a−d,9] or photoinduced electron transfer[13b] may seem feasible particularly in PPV/BBL heterojunctions and perhaps also in PPV/polyanthrazoline bilayers. We

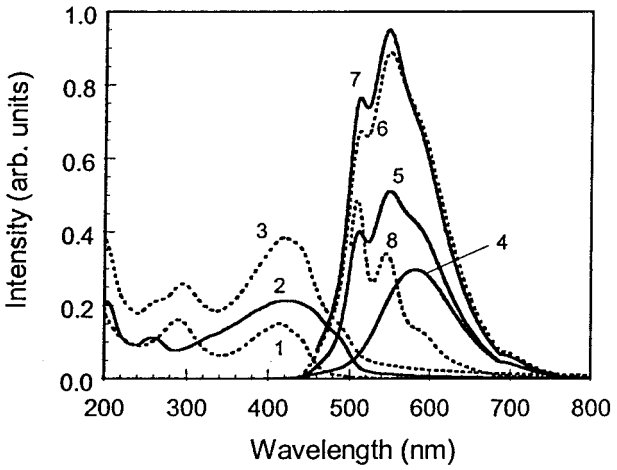

Figure 4. Optical absorption spectra of PPQ (1), PPV (2), and bilayer PPQ/PPV (3) thin films on silica substrates. PL spectra of PPQ (4, excited at 400 nm) and bilayer PPQ/PPV films (5−8, excited at 360, 400, 440, and 480 nm, respectively).

investigated these possibilities in representative bilayer heterojunctions by steady-state photoluminescence (PL) spectroscopy and in some cases also by PL decay dynamics. Optical absorption spectra of PPV/n-type polymer bilayer heterojunctions were simple superpositions of those of the component layers.

The PL emission spectra of a PPV/PPQ bilayer at different excitation wavelengths are shown in Figure 4 along with the emission spectrum of a single-layer PPQ thin film. The PL spectra corresponding to 360−440 nm excitations of the bilayer were clear superpositions of those of the component layers. Interestingly, excitation of the PPV/PPQ bilayer from the PPQ side at 480 nm, where PPQ does not absorb, gave a PL emission spectrum identical in line shape, emission maximum (510 nm), and intensity to that of a single-layer PPV thin film. Similar results were obtained in other bilayer heterojunctions. Even in the case of PPV/PBTPV where there is some evidence of exciton energy transfer from the PPV layer to the PBTPV layer, excitation-wavelength-dependent PL emission spectra were obtained. For example, excitation of the PPV/PBTPV bilayer above the absorption edge of PPV (515 nm, Table 1) gave a PL emission band that was characteristic of the single-layer PBTPV (λ_{max} = 630 nm). Excitation of the same bilayer at 400−480 nm gave PL emission bands with multipeaks due to both PPV and PBTPV. These results demonstrate that bilayer heterojunctions of fluorescent conjugated polymers exhibit *excitation wavelength tunable emission spectra*. No evidence of new emission bands that may indicate exciplex formation[9] was found in any of the bilayer heterojunctions.

Although the emission band of PPV which covers the 460−620 nm spectral range completely overlaps the absorption spectrum of BBL which covers ∼440−720 nm, no indication of exciton energy transfer was observed in the PPV/BBL bilayer heterojunction. This is consistent with the HOMO/LUMO energy levels of this pair of conjugated polymers (Figure 3). Instead, a factor of 2.1−2.3 quenching of both the luminescence of PPV and BBL was observed when the heterojunction was excited at two different wavelengths (400 and 580 nm). Photoinduced electron transfer from PPV to BBL at the junction interface is consistent with the large luminescence quenching and interface electronic structure. The PL decay dynamics obtained by exciting a single-layer

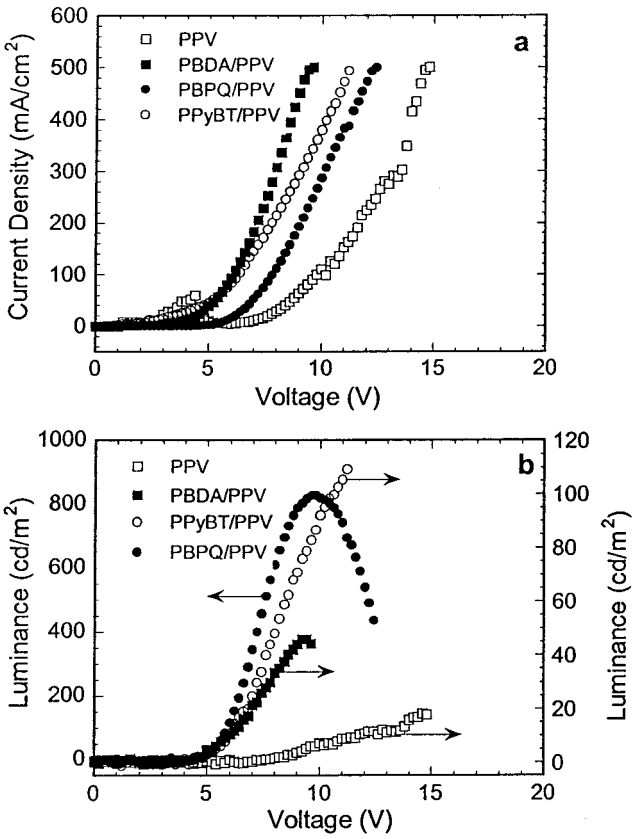

Figure 5. Current density−voltage (a) and luminance−voltage (b) characteristics of EL devices: ITO/PPV(70 nm)/Al, ITO/PPV(35 nm)/PBDA(20 nm)/Al, ITO/PPV(35 nm)/PBPQ-(30 nm)/Al, and ITO/PPV(60 nm)/PPyBT(15 nm)/Al.

PPV and a PPV/BBL bilayer at the same excitation wavelength (420 nm) and monitored at the same wavelength (540 nm) showed that the excited-state lifetime was substantially shortened in the bilayer. Whereas the single-layer PPV thin film had lifetimes of 130 and 500 ps, the PPV/BBL bilayer had lifetimes of 70 and 300 ps. These PL decay dynamics are also consistent with photoinduced electron transfer at the interface between PPV and BBL. Although the high electron affinity of BBL can be beneficial to electron injection in LEDs, efficient photoinduced electron transfer at the polymer/polymer interface and associated luminescence quenching suggest that the prospects for efficient LEDs from PPV/BBL heterojunctions are not good whereas photovoltaic cells may be more promising.

B. Enhancement of Electroluminescence of Polymer/Polymer Heterojunctions. The turn-on voltage, luminance or brightness, electrical characteristics, and electroluminescence efficiency of the 16 PPV/n-type polymer bilayer LEDs (ITO/PPV/n-type polymer/Al) were investigated in detail for comparison with the single-layer ITO/PPV/Al diode. In particular, we aimed to understand the role of the electronic structure of the polymer/polymer interface compared to other factors such as electron injection at the cathode (Al)/polymer interface.

Figure 5a shows the current−voltage ($I-V$) characteristics of three representative bilayer LEDs (PPV/PBDA, PPV/PBPQ, and PPV/PPyBT) and the single-layer PPV diode. The corresponding luminance−voltage ($L-V$) curves of these LEDs are shown in Figure 5b. For the single-layer PPV EL device (ITO/PPV(70 nm)/Al), the turn-on voltage (V_{on}) which we define as the

Table 2. Performance of Bilayer Heterojunction LEDs

device	thickness, nm	V_{on}, V	L_{max}, cd/m^2	V_{max}, V	I_{max}, mA/cm^2	efficiency, %
PPV	70	7	18 (10)[a]	15 (12)[a]	500	0.03 (0.04)[a]
PPQ/PPV	35/35	4.5	330 (324)	13 (12.5)	250	1.05 (1.20)
PPPQ/PPV	30/35	6	138	12	230	0.48
PBPQ/PPV	30/35	3.5	826	9.5	220	2.99
PBAPQ/PPV	35/35	5.5	154 (99)	12 (10.5)	410	0.30 (0.36)
PSPQ/PPV	35/35	5.5	88 (54)	14 (11.5)	500	0.14 (0.20)
PDMPQ/PPV	30/35	5.5	430 (350)	16 (14)	460	0.75 (1.41)
PTPQ/PPV	40/35	3.5	52 (27)	8 (6)	500	0.08 (0.10)
PPDA/PPV	20/35	5	46 (32)	14 (11)	460	0.08 (0.12)
PBDA/PPV	20/35	4.5	46 (26)	9.5 (7.5)	500	0.07 (0.09)
PBADA/PPV	20/35	4.5	47 (26)	12 (7.5)	490	0.08 (0.09)
PSDA/PPV	25/35	5.5	26 (14)	10 (8.5)	450	0.05 (0.05)
PDMDA/PPV	25/35	6.5	22	13	200	0.09
PTDA/PPV	25/35	6.5	19 (9)	15 (12)	500	0.03 (0.03)
PBTPV/PPV	15/60	6	48 (24)	12.5 (10)	500	0.08 (0.09)
PPyBT/PPV	15/60	5	110 (50)	11.5 (8)	500	0.18 (0.18)
BBL/PPV	30/35	*b*	*b*			

[a] The values in parentheses correspond to the current density of 220 mA/cm^2. [b] No light at all.

onset of visible light emission was 7 V (1.0×10^6 V/cm). As seen in the $I-V$ curve, the single-layer PPV diode had a current spike at ~3−5 V below the turn-on voltage. This is similar to the space charge limited transient current in organic semiconductors with traps.[35] It may be an indication of space charge accumulation at the Al/PPV interface, reflecting poor electron injection in the single-layer diode. Such an effect was not observed in the $I-V$ characteristics of all the bilayer LEDs as exemplified by those in Figure 5a. The turn-on voltage (electric field) for the three bilayer LEDs shown in Figure 5 was between 3.5 V (5.4×10^5 V/cm) for PPV/PBPQ and 5 V (6.7×10^5 V/cm) for PPV/PPyBT. The turn-on voltage (V_{on}) for all the bilayer LEDs was less than that of the single-layer PPV diode (Table 2). The reduced turn-on voltage (electric field) of the bilayer LEDs suggests improved electron injection and transport compared to the single-layer PPV diode.

The luminance or brightness of the bilayer LEDs was also substantially enhanced compared to the single-layer PPV diode, as exemplified in Figure 5b. The maximum luminance (L_{max}) of the ITO/PPV/Al diode was 18 cd/m^2 at 15 V (2.1×10^6 V/cm). The L_{max} values for the PPV/PBDA and PPV/PPyBT bilayer LEDs at the same voltage were 47 and 110 cd/m^2, respectively. The brightest bilayer LED was the PPV/PBPQ heterojunction with an L_{max} of 820 cd/m^2 (Figure 5b, Table 2). Other very bright bilayer LEDs include PPV/PPQ and PPV/PDMPQ with L_{max} of 330−430 cd/m^2 (Table 2).

The LED performance data, including the turn-on voltage (V_{on}), L_{max} with corresponding operating voltage (V_{max}), current density (I_{max}), and EL efficiency are summarized in Table 2 for the 16 bilayer heterojunctions and the single-layer PPV. To facilitate easy comparison, the luminance, operating voltage, and EL efficiency corresponding to a current density of 220 mA/cm^2 are also given in Table 2. For example, at this current density the luminance of the single-layer PPV and the bilayers PPV/PDMPQ and PPV/PBPQ was 10, 350, and 826 cd/m^2, respectively, showing enhancements of 35−83 times. In general, the luminance of the bilayer heterojunctions varied substantially among the different classes of n-type conjugated polymers as shown in Figure 3. Bilayers containing polyquinolines (PQs) were the brightest and most enhanced, followed by the polybenzobisthiazoles (PBTs), whereas the polyanthrazolines (PATs) resulted in the smallest enhancement relative to the reference single-layer PPV diode. Light emission was not obtained from the PPV/BBL diode.

The observed trends in the luminance data were also evident in the EL efficiency data (Table 2). The PPV/PBPQ and PPV/PDMPQ bilayer diodes had EL efficiencies of 3% and 1.4% photons/electron, respectively. Except for the PPV/PTPQ bilayer which was more efficient by a factor of 2.7, all the PPV/polyquinoline heterojunctions had EL efficiency enhancement of 5−100 times relative to the single-layer PPV diode. Bilayers of PPV/polybenzobisthiazoles and PPV/polyanthrazolines had EL efficiency enhancements of factors of 3−6 and 2−3, respectively. No light emission was observed from the PPV/BBL LED. As electron transport layers for PPV-based LEDs, these results show that the polyquinolines as a class, and particularly the members PPQ, PDMPQ, and PBPQ, are the best and superior to prior reported materials such as the polyoxadiazoles,[12b] poly(phenylquinoxalines),[12d] and polypyridine.[12g]

The observed enhancement of EL efficiency and LED brightness in these bilayer heterojunctions, particularly their variation with n-type polymer structures, are very difficult to understand in terms of improved electron injection and transport. Insertion of an n-type polymer or electron transport layer (ETL) between PPV and aluminum cathode is supposed to improve LED performance by reducing the barrier to electron injection at the cathode ΔE_c ($= \Phi_c - EA$) (Figure 1b) through its higher electron affinity relative to PPV.[12c] However, our finding with the series of 16 n-type polymers is that those with the highest EA values had the worst bilayer LED performance relative to the PPV single layer (Tables 1 and 2). For example, the ITO/PPV/BBL/Al diode has an essentially ohmic contact at the BBL/Al interface with an almost perfect match of EA (4.0 eV) to the work function of Al (~4.0−4.3 eV).[19b] Yet this bilayer had no light emission and hence was worse than the single-layer PPV diode. From these results we conclude that because the bilayer LED performance does not improve with increasing electron affinity but instead decreases, the size of the electron injection barrier at the aluminum/n-type polymer interface is not an important factor in the observed variation of EL efficiency and luminance with bilayer heterojunction *composition*. A likely reason for this is that electron injection at the Al/n-type polymer interface is equally efficient, regardless of the specific polymer in the series, due to a reaction at the interface which mediates the injection process. Such metal/conjugated polymer interfacial reactions are known to always occur upon evaporative deposition of metal atoms onto a conjugated

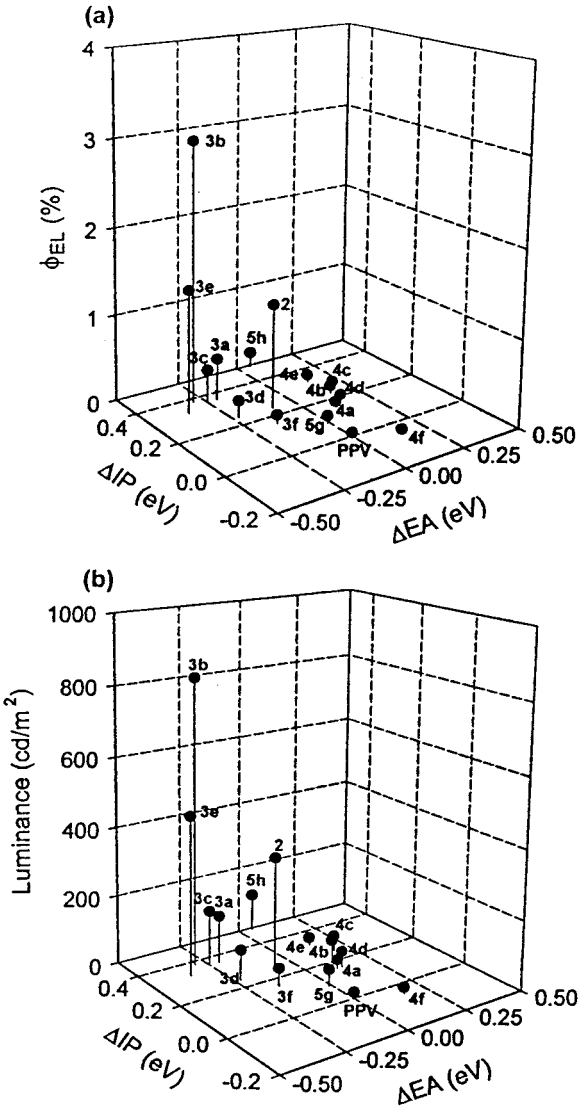

Figure 6. A 3-D plot of (a) the EL efficiency (ϕ_{EL}) and (b) the maximum luminance (L_{max}) of the bilayer heterojunction LEDs and the PPV single-layer diode as a function of ΔEA and ΔIP.

polymer.[21] In the case of the series of n-type polymers under investigation here (Chart 1), their electron-rich heteroatoms can be expected to make formation of an interface Al/polymer reaction product more facile. We also expect that such an interfacial aluminum/polymer complex would be similar in structure and function to an *n-type doped polymer*, facilitating efficient electron injection regardless of the electron affinity value of the polymer. We propose that the electronic structure of the polymer/polymer interfaces rather than electron injection at the Al/polymer interface is the key to understanding the observed electroluminescence enhancement and trends in these bilayer heterojunctions as discussed below.

C. Roles of Polymer/Polymer Interfaces in Heterojunction LEDs. A critical examination of the above electroluminescence efficiency (ϕ_{EL}) and luminance data suggests that they are strong functions of both ΔEA and ΔIP which characterize the electronic structure of the polymer/polymer interface (Figure 1b). A 3-D plot of ϕ_{EL} or L_{max} as a function of the variables ΔEA and ΔIP best quantifies these dependencies as shown in Figure 6. A combination of energetic barrier to hole transfer (ΔIP > 0) and favorable electron transfer (ΔEA < 0) at the interface appears to be the necessary requirement for enhanced EL emission in the bilayer LEDs. On this basis all the observed trends of EL efficiency and diode luminance in the bilayer heterojunctions can be fully rationalized.

The interface energetics of PPV/polyquinoline heterojunctions is such that there is no barrier to electron transfer from the PQs to the PPV layer while there is about a 0.16−0.38 eV barrier to hole transfer across the interface from the PPV layer. Provided that the alignment of the LUMO levels at the interface favors electron transfer (ΔEA < 0) for a given bilayer, then the largest energy barrier to hole transfer gives the best EL performance as exemplified in PPV/PDMPQ and PPV/PBPQ, which have ΔIP of 0.32−0.38 eV and the highest efficiencies and brightness among the polyquinolines. Although the polybenzobisthiazoles (PBTs) have 0.09−0.49 eV barrier to hole transfer from PPV, they also have small barriers to electron transfer (ΔEA = 0.05 eV for PPyBT) which appears to account for the poorer performance of PPV/PBT LEDs compared to the polyquinolines. The superior EL results for PPyBT relative to PBTPV can be traced to its larger hole confinement energy (ΔIP = 0.49 eV). The polyanthrazolines combine unfavorable barrier to interface electron transfer (ΔEA ∼0.1−0.18 eV) with small barriers to hole transfer, resulting in only marginal EL enhancement. In fact, in PPV/PTDA there is no barrier to hole transfer, and not surprisingly no EL enhancement was observed compared to the PPV single layer. Although PPV/BBL bilayer LED has a large barrier to hole transfer (ΔIP = 0.8 eV), however, it also has a large barrier to electron transfer (ΔEA = 1.29 eV) at the interface which precludes any light emission.

To understand why the energetics of the polymer/polymer interface can dominate the EL efficiency ϕ_{EL} and luminance, we consider the main factors that determine EL diode efficiency. In organic LEDs, in general, $\phi_{EL} = \gamma\eta\phi_{PL}$ where γ is the charge injection efficiency, η is the efficiency of singlet exciton generation from electron−hole recombination, and ϕ_{PL} is the fluorescence quantum yield of the emissive polymer layer.[1a,36] Focusing on the emissive PPV layer which is a constant in all the bilayer heterojunctions, one sees that ϕ_{PL} does not vary with heterojunction composition. As previously discussed, since the bilayer LED performance (e.g., ϕ_{EL}) did not increase with increasing electron affinity, the electron injection efficiency γ is likely to be very high and about the same in all the heterojunctions. Thus, what varies widely in these heterojunctions is the singlet exciton generation efficiency of charge recombination η. For example, although the charge injection efficiency γ of the ITO/PPV/BBL/Al diode is near unity because of ohmic contacts, the fact that $\phi_{EL} \sim 0$ can be understood to arise from the negligible radiative recombination ($\eta \sim 0$) due to interfacial photoinduced electron transfer and charge separation facilitated by the interfacial electronic structure.

The electric field dependence of electron−hole recombination and the competing process of exciton (electron−hole) dissociation in these bilayer heterojunctions, and hence η, can also be expected to depend on the composition and interfacial electronic structure of the bilayer.[39] An unusual maximum appearing in the luminance−voltage curves of the heterojunction LEDs provided additional evidence of the critical role of the polymer/polymer interface in the net η and diode performance.

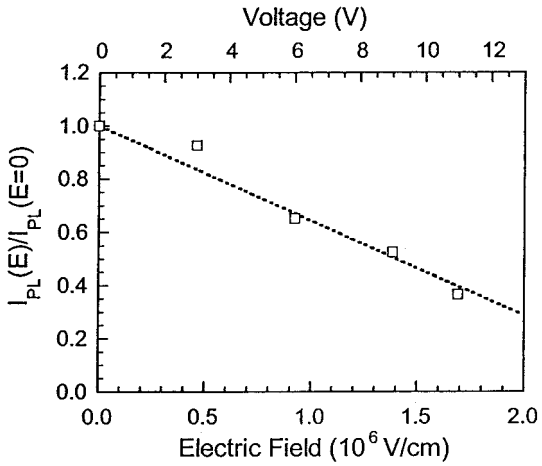

Figure 7. Electric-field-induced quenching of PL in the ITO/PPV/PBPQ/Al diode under reverse bias. The excitation wavelength was 470 nm.

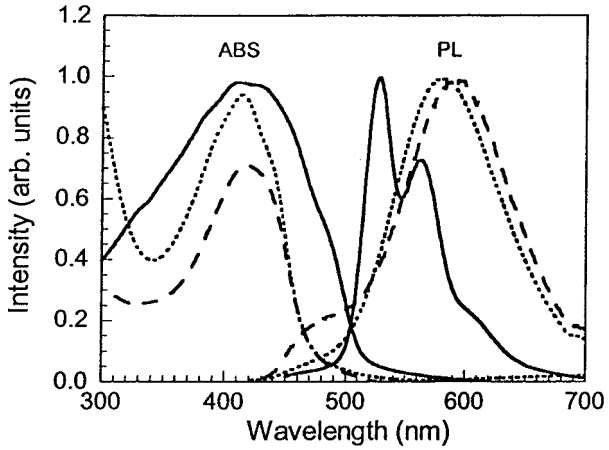

Figure 8. Optical absorption (ABS) and photoluminescence (PL) spectra of PPV (solid line), PPQ (dotted line), and PSPQ (dashed line) thin films on silica substrates. The excitation wavelength was 400 nm for all three polymers.

The luminance of the previously discussed ITO/PPV/PBPQ/Al diode was found to have a maximum at 9.5 V (Figure 5b). Above this bias voltage, the luminance decreased with increasing voltage even though the current was increasing monotonically. The bias voltage (electric field) where the luminance peaked varied with bilayer composition (Table 2). Such a peak in the luminance−voltage curve has not been observed in either single-layer diodes or bilayer LEDs involving a nonconjugated polymer layer.[1,30a] The most likely explanation for this peak in the luminance−voltage curve is electric field-induced quenching of luminescence due to increasing electron−hole (exciton) dissociation with increasing electric field.[15b,39] We applied electric field modulated PL spectroscopy[15b] to investigate the ITO/PPV/PBPQ/Al diode under reverse bias voltages that does not give rise to EL emission. The relative PL intensity, $I_{PL}(E)/I_{PL}(0)$, is seen to decrease with increasing electric field, reaching a value of 0.4 at $\sim 1.6 \times 10^6$ V/cm (Figure 7). This result shows that there is a 60% quenching of luminescence by a high electric field (>10 V). The efficiency of charge photogeneration at the polymer/polymer interfaces at comparable electric fields is known to be strongly dependent on the bilayer composition and particularly the interface electronic structure (ΔEA, ΔIP).[5]

D. Voltage-Tunable Multicolor Electroluminescence from Bilayers. A key observation in our preliminary[8a,b] and present studies of the bilayer heterojunction LEDs of the type ITO/PPV/n-type polymer/Al (Figure 1b) was the dramatic effect of the layer thicknesses on the EL color and its voltage dependence. We have found that if the thickness of the PPV layer was in the range 60−120 nm and that of the n-type polymer was thinner, green light emission which is characteristic of the single-layer PPV diode was obtained at all applied bias voltages. Similarly, an emissive n-type polymer layer of 60−120 nm in combination with a thinner PPV layer always resulted in orange or red emission which is characteristic of the n-type polyquinoline layer at all bias voltages. In contrast to these conventional *single-color* polymer LEDs, we have found that the bilayer heterojunction LEDs exhibit novel *voltage-dependent multicolor EL emission* if the layer thicknesses are in the range 25−50 nm. In the following, results of studies aimed at the understanding of the mechanisms of such a voltage-tunable EL emission from the bilayer heterojunctions, size effects, and the roles of the polymer/polymer interfaces are presented and discussed.

The photoluminescence (PL) and optical absorption spectra of single-layer thin films of PPV, PPQ (**2**), and PSPQ (**3d**) are shown in Figure 8. The PPV thin film has a broad absorption band with a peak at 408 nm and absorption edge at ∼515 nm. The PL spectrum of PPV is highly structured with vibronic peaks at 528 and 559 nm. The PPQ thin film has an absorption peak at 414 nm and a PL emission peak at 578 nm. In the case of the PSPQ thin film, the absorption and PL emission peaks are at 414 and 590 nm, respectively. The photophysical data (absorption maxima λ_{max}^{ABS}, absorption edge gap E_g^{opt}, and PL emission maxima λ_{max}^{PL}) for all the polymers are collected in Table 1. The photophysical data, exemplified by those in Figure 8, show that there is little or no overlap between the absorption of PPV and the emission of the n-type polymers listed in Table 1. Therefore, light emitted from the n-type polymer layer in a ITO/PPV/n-type polymer/Al diode can exit from the ITO side without any significant reabsorption by the PPV layer. This fact together with the different emission colors of the p-type (PPV) and n-type polymer layers facilitated the observed multicolor EL emission from the bilayer heterojunction diodes.

Voltage-tunable multicolor EL emission of the bilayer heterojunction LEDs is exemplified by the ITO/PPV(35 nm)/PPQ(35 nm)/Al diode which switches reversibly from red (7 V) to yellow (9 V) and to green (12 V). These multicolor switchings by the applied bias voltage were observed visually and also by EL microscopy. Typical EL micrographs of a color tunable PPV/PPQ diode are shown in Figures 9 and 10. In addition to the three main colors (red/orange ↔ yellow ↔ green) (Figure 9) seen at 7, 9, and 12 V, continuous variation of the bias voltage within the range 6−13 V gives rise to more than 8 shades of color (Figure 10). The dark spots seen in the EL micrographs are very similar to those previously observed in organic LEDs[37] and are nonemissive areas due to defects. An important difference between the dark spots seen here in the EL micrographs of polymer/polymer bilayer LEDs and those reported in small molecule organic/organic LEDs[37] is that the size and distribution of dark spots in the present diodes (Figures 9 and 10) do not grow with increasing voltage or time.

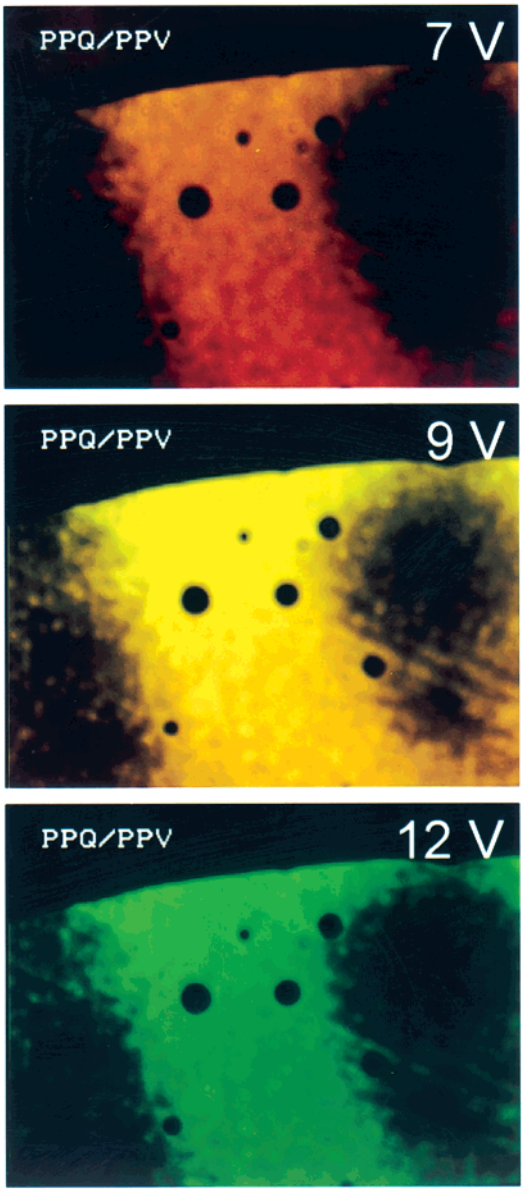

Figure 9. EL micrographs (×40) of the ITO/PPV(35 nm)/PPQ-(35 nm)/Al diode at 7, 9, and 12 V. The corresponding EL spectra are shown in Figure 11b.

This suggests that the dark spots seen here are preexisting defects associated with the device fabrication and are not evidence of EL diode degradation sites.

The EL spectra of single-layer ITO/PPV/Al and ITO/PPQ/Al diodes are shown in Figure 11a. The single-layer PPV diode emits green light with peaks at 527 and 559 nm; the single-layer PPQ diode emits orange/red light with a broad band and peak at 589 nm. The voltage-tunable EL spectra corresponding to the EL micrographs of Figure 9 for the PPV/PPQ bilayer diode are shown in Figure 11b. The EL spectrum at 7 V has a peak at 615 nm, showing the characteristic red/orange PPQ emission. The EL spectrum at 9 V has a shoulder at 530 nm and a peak at 570 nm, which is completely different from that of either component. The 9-V EL spectrum is actually a superposition of those of the component polymers as demonstrated by its deconvolution which showed 25% contribution from the PPV layer and 75% from the PPQ layer. The EL spectrum at 12 V has peaks at 529 and 566 nm. Although the 12 V EL spectrum and green color are very close to the single-layer PPV diode, the EL spectrum has some contribution from the PPQ layer as shown in the simulation of Figure 11c. These results clearly show that muticolor EL emission from the bilayer heterojunction diodes originates from the mixing of light colors emitted from the two different emissive layers.

The performance of the voltage-tunable multicolor ITO/PPV/PPQ/Al diode was also substantially enhanced compared to the single-layer devices. The current−voltage and luminance−voltage characteristics of this color-tunable diode are shown in Figure 12. The turn-on voltage was 4.5 V. The maximum luminance was 324 cd/m^2 at a current density of 220 mA/cm^2 (12.5 V), and the EL efficiency was 1%. These results show that voltage-tunable multicolor light emission from the bilayer heterojunction diodes is both efficient and bright.

Similar voltage-tunable multicolor EL emission was observed in many other ITO/PPV/polyquinoline/Al diodes. Typical voltage-tunable EL spectra of PPV/PBAPQ and PPV/PSPQ diodes are shown in Figure 13. For the PPV/PBAPQ diode, the color switching was orange (6−9 V) ↔ yellow (12 V) ↔ green (15 V); the color switching in the PPV/PSPQ diode was orange/red (6 V) ↔ yellow (9 V) ↔ green (12 V). Interestingly, in the case of the PPV/PBTPV diode the low-voltage (5 V) color was green and the highest-voltage (19 V) color was orange/red. The detailed results for these and other bilayer heterojunction LEDs are summarized in Table 3.

The main features of these results suggest that the basic mechanism of voltage-tunable multicolor EL emission is the spatial variation of the recombination and emission zone within the bilayer LED. If recombination and emission occur exclusively in one layer, the LED color obtained is that characteristic of that layer. However, if recombination and emission occur in both layers, the EL color results from a physical mixing of those of the two components of the heterojunction LED. The spatial location of charge recombination and hence where light emission occurs and ultimately the EL color of a bilayer heterojunction LED of the type anode/p-type/n-type/cathode is thus controlled by charge transfer across the polymer/polymer interface. All the experimental results suggest that the nature of the charge transfer at a p/n polymer/polymer heterojunction interface can be one of three types: (i) *unipolar electron transfer*, (ii) *unipolar hole transfer*, and (iii) *combined unipolar* (at low electric fields) and *bipolar* (at high electric fields) *charge transfer*. These interfacial charge-transfer processes are controlled by three main interrelated factors: (a) the sizes of the layers forming the heterojunction interface, (b) the bias voltage or electric field, and (c) the electronic structure or energetics (ΔEA, ΔIP) of the interface. To understand how these factors control interfacial charge transfer and EL color of a bilayer LED, we consider the physical parameters defined in Figure 14.

The p-type and n-type layer thicknesses of a bilayer diode are denoted L_p and L_n, respectively. To achieve EL emission, charge carriers injected at the electrodes migrate under the influence of electric field until they are trapped, or they encounter energy barriers (ΔEA, ΔIP) at the interface, or they recombine. The *range* of a charge carrier injected into a semiconductor is the mean distance traveled before trapping or recombination.[16a,38] The ranges of electrons (x_n) and holes (x_h) in the semiconducting polymer heterojunction are illustrated

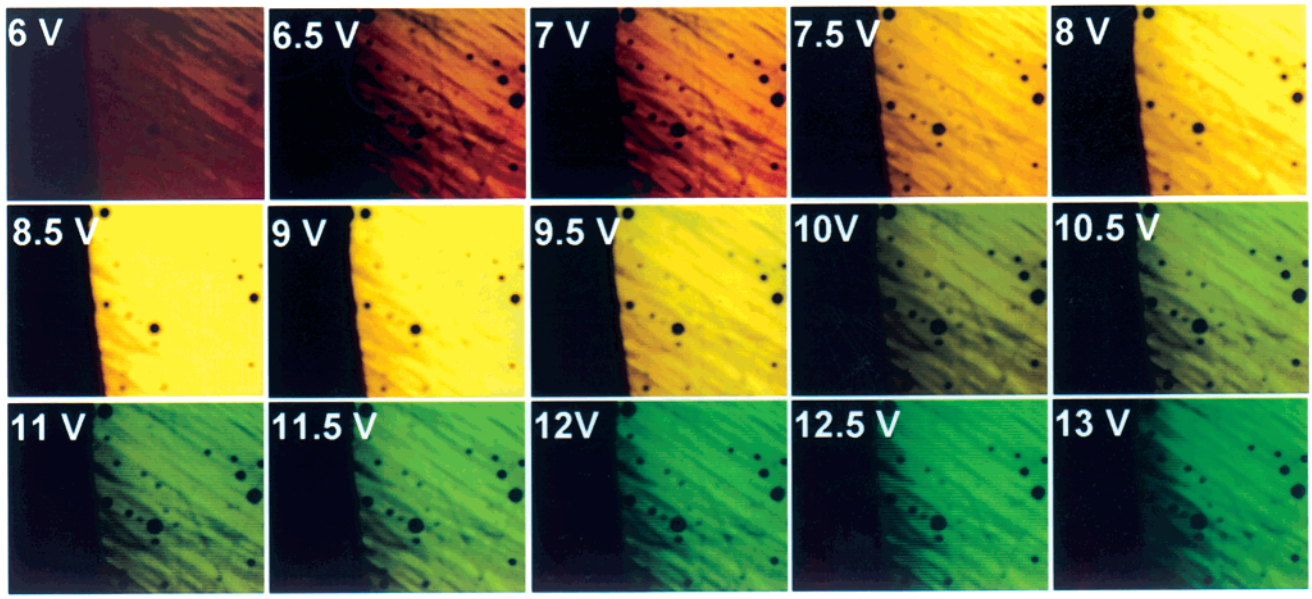

Figure 10. EL micrographs (×30) of the ITO/PPV(35 nm)/PPQ(35 nm)/Al diode at various bias voltages showing continuous voltage tunability of EL emission color.

in Figure 14. The range of holes in a semiconducting polymer is approximately the product of hole mobility (μ_h), carrier lifetime (τ_h), and electric field (E): $x_h = \mu_h\tau_h E$.[16a] Similarly, the range of electrons is approximately given by $x_e = \mu_e\tau_e E$. These ranges are for the respective majority carrier in the semiconductor. Although the ranges of electrons and holes in semiconducting polymers are rarely known, they are expected to be in the nanoscale region. We propose that the observed *finite size effects* on the EL emission of the bilayer heterojunctions arise from the limitations imposed on charge transport by *the charge carrier ranges* in semiconducting polymers. Depending on the relative layer thicknesses (L_p, L_n) of a bilayer LED and the applied electric field, two limiting situations corresponding to *unipolar* charge transfer across the interface arise. If the n-layer thickness is less than the electron range ($L_n < x_e$) and the p-layer thickness is greater than the hole range ($L_p > x_h$), unipolar electron transfer across the polymer interface occurs, and EL emission from only the p-layer is observed at all bias voltages. Heterojunction LEDs with relatively thick PPV layers (see Table 3) fall into this category. On the other hand, if the n-layer thickness is greater than the electron range ($L_n > x_e$) and the p-layer thickness is less than the hole range ($L_p < x_h$), unipolar hole transfer across the polymer/polymer interface occurs, and EL emission from only the n-layer is observed at all bias voltages. This is the case of the ITO/PPV(25 nm)/PPQ(67 nm)/Al diode which emits orange/red, which is characteristic of PPQ, at all bias voltages.

The most interesting case of combined unipolar and bipolar charge transfer across the polymer/polymer interface and associated voltage-tunable multicolor EL emission arises when both the n-layer and p-layer thicknesses are comparable to or less than the electron and hole ranges ($L_n \leq x_e$, $L_p \leq x_h$). At low voltages either unipolar hole transfer, and hence emission from the n-type layer, or unipolar electron transfer and emission from the p-type layer is observed depending on the composition of the bilayer heterojunction. At high voltages bipolar charge transfer takes over, facilitating EL emission from both layers. The PPV(25 nm)/PBTPV(35 nm) diode exemplifies the switch from unipolar electron transfer to bipolar charge transfer with green (5 V) ↔ orange/red (19 V) reversible switching of colors. All the other bilayer LEDs switch from unipolar hole transfer to bipolar charge transfer similar to the previously discussed PPV(35 nm)/PPQ(35 nm) diode (Table 3). The reason for this is likely due to the much higher mobility of holes in PPV than the mobility of electrons in the n-type polymers ($\mu_h > \mu_e$), except perhaps in PBTPV. The strong electric field (bias voltage) dependence of EL color (spectra) arises mainly from the strong and sensitive dependence of the charge carrier ranges in semiconducting polymers on electric field since both the mobility (μ_i) and carrier lifetime (τ_i) appearing in the expression $x_i = \mu_i\tau_i E$, where the subscript i denotes either h (holes) or e (electrons), are also strong functions of the electric field.

The observed critical dependence of the electronic and optical properties (e.g., EL emission spectrum, efficiency, and luminance) of polymer/polymer heterojunctions on the relative nanoscale sizes of the bilayer components constitutes an interesting class of *finite size effects* which are yet to be fully explored in *organic semiconductors*. In the present context we see that there is a coupling between the properties of polymer/polymer interfaces (e.g., ΔEA, ΔIP) which can be achieved through molecular design and synthesis and those due to *finite size effects* which must be controlled through nanoscale materials processing.

E. Design and Applications of Multicomponent Organic EL Systems. The above results on bilayer semiconducting polymer heterojunctions demonstrate the potential of multicomponent EL polymer systems for developing efficient and bright light-emitting devices. The novel feature of *continuous* voltage-tunable multicolor emission from the heterojunction LEDs suggests full-color displays, color-switchable panels, and other applications. Pixels of multicolors could be easily fabricated by using conventional photolithography, microcontact printing, or ink-jet printing techniques.[1] Although the present PPV/polyquinoline heterojunctions had voltage-tunable colors in the range red ↔ yellow ↔ green, other bilayer (red + blue, blue + green) and

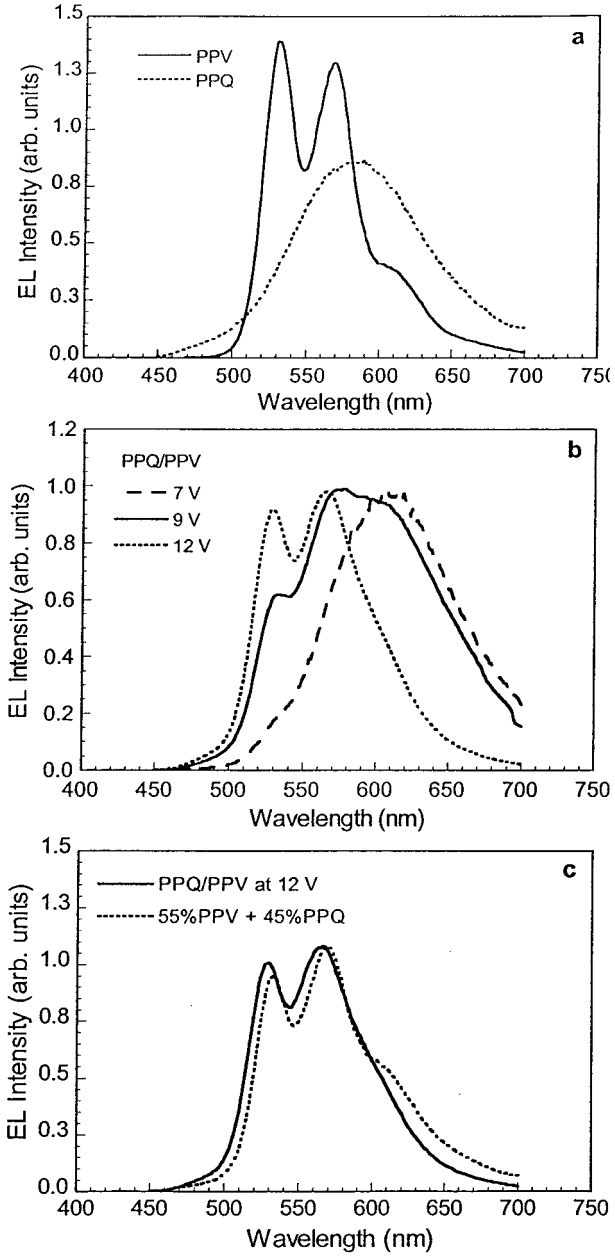

Figure 11. (a) EL spectra of single-layer ITO/PPV(70 nm)/Al diode at 8 V and ITO/PPQ(30 nm)/Al diode at 8 V. (b) EL spectra of ITO/PPV(35 nm)/PPQ(35 nm)/Al diode at forward bias voltages of 7, 9, and 12 V. (c) Deconvolution of the EL spectrum of ITO/PPV(35 nm)/PPQ(35 nm)/Al diode at 12 V.

trilayer (red + green + blue) heterojunctions involving p-type polymers such as poly(*p*-phenylene) (PPP)[17] and polyfluorene (PF)[18] can readily extend the accessible multicolors througout the CIE diagram. The combination of three EL polymers having three different primary colors (red, green, blue) could also be achieved in a bilayer heterojunction LED if one of the layers is a binary blend. In addition to blue ↔ green ↔ red type of color switching, such heterojunction LEDs may also be capable of white light emission.

In light of the present results, the goals of molecular design and synthesis of semiconducting polymers for EL devices should include the electronic structure of polymer/polymer interfaces in addition to high solid-state PL efficiency and good charge transport. For single-color LEDs, this means that if the p-type layer of a bilayer heterojunction is to serve as the emissive layer, the

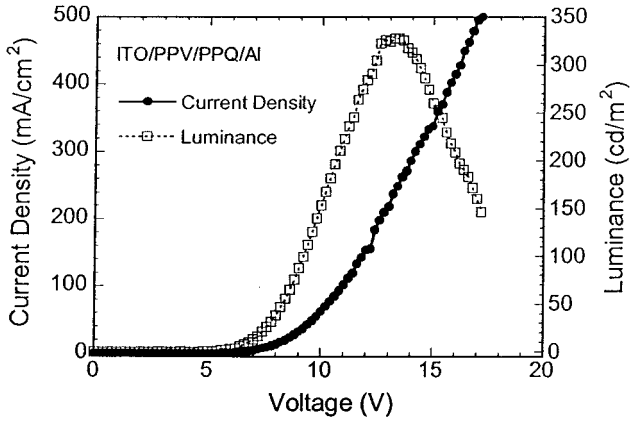

Figure 12. Current density−voltage and luminance−voltage characteristics of the color-tunable ITO/PPV(35 nm)/PPQ(35 nm)/Al diode.

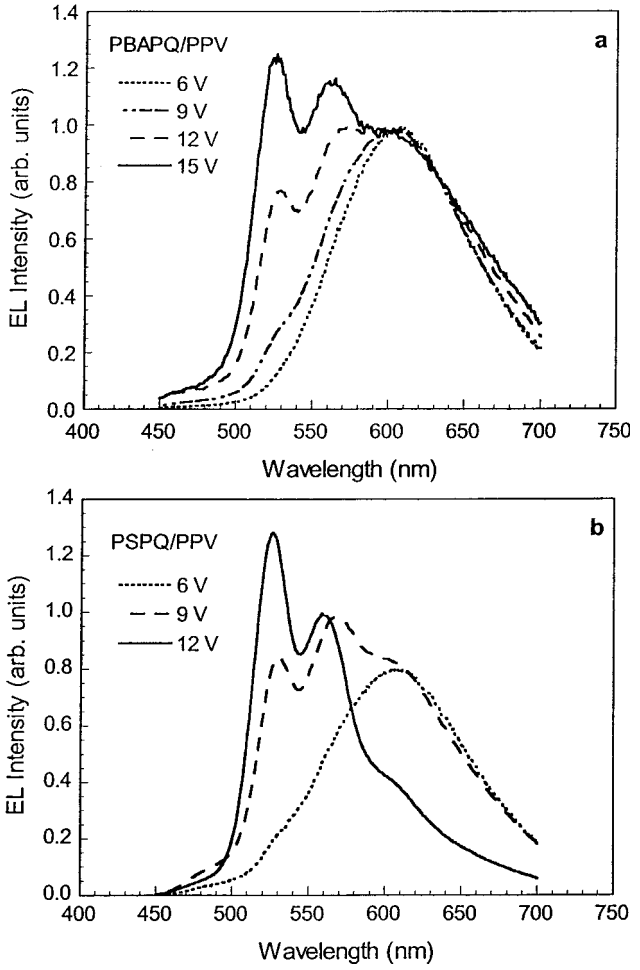

Figure 13. EL spectra of (a) the ITO/PPV(35 nm)/PBAPQ-(35 nm)/Al diode at 6, 9, 12, and 15 V and (b) the ITO/PPV(35 nm)/PSPQ(35 nm)/Al diode at 6, 9, and 12 V.

desired interfacial electronic structure is $\Delta EA < 0$ and $\Delta IP \gg 0$. Similarly, the EL emission of the n-type layer would be maximized if the bilayer heterojunction is such that $\Delta IP < 0$ and $\Delta EA \gg 0$. Coupled to these molecular parameters (IP/HOMO, EA/LUMO) is the choice and manipulation of the nanoscale layer thicknesses (L_p, L_n). If either L_p or L_n is relatively large compared to the charge carrier ranges in the component semiconducting polymers, single-color LEDs would be obtained. If the relative layer thicknesses are comparable to the charge

Table 3. Single-Color and Voltage-Tunable Multicolor Polymer Heterojunction LEDs

device	thickness (nm)	V_{on} (V)	EL colors and peaks[a] at applied voltages
PPV	70	7	green (531/564 nm)
PPQ/PPV	35/35	4.5	red/orange (6 V, 607 nm) ↔ yellow (9 V, 578−600 nm) ↔ green (12 V, 566/529) ↔ green (>12 V, 526/561 nm)
	67/25	10	orange/red (at all voltages, 610 nm)
	40/25	7	orange/red (8−10 V, 614 nm) ↔ green (13−20 V, 507/544 nm)
	33/62	10	orange (10−15 V, 592 nm) ↔ green (18−20 V, 508/544/588 nm)
	33/117	14	green (548 nm)
PPPQ/PPV	85/25	15	orange (580 nm)
	35/25	8	yellow/orange (10 V, 572 nm) ↔ green (20 V, 511/549 nm)
	35/60	10	green (508/544 nm)
	30/35	6	green (528/559 nm)
PBPQ/PPV	30/35	3.5	green (3.5−5 V, 563/528 nm, >5 V, 528/563 nm)
	40/25	10	yellow/orange (10 V, 566 nm) ↔ green (20 V, 510/544 nm)
	50/25	12	orange (580 nm)
PBAPQ/PPV	35/35	5.5	orange (6−9 V, 600 nm) ↔ yellow (12 V, 530−600 nm) ↔ green (15 V, 526/561 nm)
PSPQ/PPV	35/35	5.5	orange/red (6 V, 606 nm) ↔ yellow (9 V, 567/530 nm) ↔ green (12 V, 530/558 nm)
PPyBT/PPV	15/60	5	green (510/545 nm)
	30/25	6.5	green (510/545 nm)
	40/25	10	orange (13 V, 510−700 nm band) ↔ green (15 V, 544 nm)
PBTPV/PPV	15/60	6	green (510/545 nm)
	35/25	3.5	green (5 V, 510/550 nm) ↔ orange/red (19 V, 572 nm)
	50/25	12	red/orange (620 nm)

[a] If two peaks were shown in EL spectra (p1/p2 nm), p1 is the one with higher intensity.

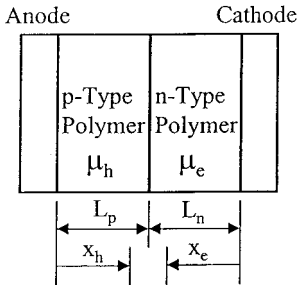

Figure 14. Schematic illustration of layer thicknesses (L_n, L_p) and charge carrier ranges (x_n, x_h) in p-type/n-type polymer heterojunction LEDs.

carrier ranges, voltage-tunable multicolor EL emission is to be expected. Clearly, control of the finite size effects in heterojunction LEDs is largely through appropriate nanoscale materials processing. The relative sizes of layered polymer/polymer heterojunction devices can be readily controlled during the fabrication process. However, the scale of phase separation in blends of EL polymers is more difficult to control, particularly at the nanoscale level.[7] Although microphase separation of block copolymers generally results in nanostructures and hence would ideally allow the control of finite size effects, there are currently only few examples of luminescent block conjugated polymers[15] for possible use in LEDs.

The ability to predict the EL emission color of a multicomponent polymer system from those of the component EL spectra also depends on the extent of any intermolecular photophysical processes such as energy transfer,[10] exciplex formation,[9] or photoinduced electron transfer.[13] Tunable multicolor EL emission from the bilayer heterojunction LEDs investigated here was best controlled in the absence of any intermolecular photophysical processes. Bilayers with significant photoinduced electron transfer, such as the PPV/BBL system, had very poor light-emitting properties. Knowledge of the electronic structures (IP/HOMO, EA/LUMO) and photophysical properties of the components can be used to estimate the likelihood of intermolecular photophysical processes across the polymer/polymer interfaces in layered thin films, phase-separated blends, or microphase-separated block copolymers. Although energy transfer and exciplex formation are undesirable complications in tunable multicolor EL polymer systems, each can separately be used to enhance emission in *single-color* devices.[9,10,14]

Conclusions

Our systematic investigation of the electroluminescence of bilayer heterojunctions of PPV (p-type layer) and a series of n-type conjugated polymers, with electron affinities in the 2.36−4.0 eV range and ionization potentials in the 5.06−5.90 eV range, has shown that the electronic structure of the polymer/polymer interface plays a more important role in EL efficiency and diode brightness than injection barrier at the cathode/polymer interface. For a p-type emissive layer, such as PPV, our results show that both efficiency and diode brightness are maximized when the energetics of the bilayer heterojunction interface favors electron transfer ($\Delta EA < 0$) while disfavoring hole transfer ($\Delta IP > 0$). A similar requirement of favorable hole transfer ($\Delta IP < 0$) and unfavorable electron transfer ($\Delta EA > 0$) across the interface of a bilayer LED with an n-type emitter also follows. Therefore, although synthesis of n-type (electron transport) polymers with large electron affinities is of broad interest per se, for applications in LEDs the absolute LUMO/EA and HOMO/IP energy levels of the n-type polymer are not the most critical, but these energy levels *relative* to those of the p-type (hole transport) polymer in a heterojunction are. Our results have demonstrated that the series of n-type conjugated polymers investigated, including the polyquinolines, polyanthrazolines, and polybenzobisthiazoles, are good electron transport materials, but the polyquinolines gave the best results with PPV.

Voltage-tunable multicolor emission was observed in bilayer heterojunction LEDs containing emissive p-type and n-type layers with sizes in the range 20−50 nm. However, bilayer heterojunction LEDs of similar composition but having thicker layers had conventional

single-color emission. These results show that the electronic and optical properties of polymer/polymer heterojunctions critically depend on the relative sizes of the bilayer components. These *finite size effects* originate from the small *charge carrier ranges* in semiconducting polymers. Our observations on the roles of polymer/polymer interfaces and on the associated finite size effects on the electroluminescence of bilayer heterojunctions are expected to be applicable to other multicomponent conjugated polymer systems.

Acknowledgment. This research was supported by the Office of Naval Research, the National Science Foundation (CHE-9120001), and the Army Research Office MURI (DAAD19-99-1-0206).

Supporting Information Available: Text giving full names of all polymers in Chart 1, text describing photophysical processes at the polymer/polymer interfaces, figures showing optical absorption spectra, PL spectra, and PL decay dynamics of bilayer polymer/polymer heterojunctions, and figures showing current−voltage and luminance−voltage characteristics of bilayer polymer heterojunction LEDs from which Figure 6 was generated. This material is available free of charge via the Internet at http://pubs.acs.org.

References and Notes

(1) (a) Friend, R. H.; Gymer, R. W.; Holmes, A. B.; Burroughes, J. H.; Marks, R. N.; Taliani, C.; Bradley, D. D. C.; Dos Santos, D. A.; Bredas, J. L.; Logdlund, M.; Salaneck, W. R. *Nature* **1999**, *397*, 121−128. (b) Kraft, A.; Grimsdale, A. C.; Holmes, A. B. *Angew. Chem., Int. Ed. Engl.* **1998**, *37*, 402−428.

(2) (a) Tarkka, R. M.; Zhang, X.; Jenekhe, S. A. *J. Am. Chem. Soc.* **1996**, *118*, 9438−9439. (b) Eichen, Y.; Nakhmanovich, G.; Gorelik, V.; Epshtein, O.; Poplawski, J. M.; Ehrenfreund, E. *J. Am. Chem. Soc.* **1998**, *120*, 10463−10470. (c) Burn, P. L.; Kraft, A.; Baigent, D. R.; Bradley, D. D. C.; Brown, A. R.; Friend, R. H.; Gymer, R. W.; Holmes, A. B.; Jackson, R. W. *J. Am. Chem. Soc.* **1993**, *115*, 10117−10124. (d) Zhang, X.; Shetty, A. S.; Jenekhe, S. A. *Acta Polym.* **1998**, *49*, 52−55.

(3) (a) Tessler, N.; Denton, G. J.; Friend, R. H. *Nature* **1996**, *382*, 695−697. (b) Hide, F.; Diaz-Garcia, M. A.; Schwartz, B. J.; Andersson, M. R.; Pei, Q. B.; Heeger, A. J. *Science* **1996**, *273*, 1833−1836. (c) Wegmann, G.; Giessen, H.; Greiner, A.; Mahrt, R. F. *Phys. Rev. B: Conden. Matter* **1998**, *57*, R4218−R4221.

(4) (a) Antoniadis, H.; Hsieh, B. R.; Abkowitz, M. A.; Jenekhe, S. A.; Stolka, M. *Synth. Met.* **1994**, *62*, 265−271. (b) Halls, J. J. M.; Walsh, C. A.; Greenham, N. C.; Marseglia, E. A.; Friend, R. H.; Moratti, S. C.; Holmes, A. B. *Nature* **1995**, *376*, 498−500. (c) Yi, S.; Jenekhe, S. A. Manuscript in preparation.

(5) (a) Zhang, X.; Jenekhe, S. A.; Perlstein, J. *Chem. Mater.* **1996**, *8*, 1571−1574. (b) Zhang, X.; Alanko, A. K.; Jenekhe, S. A. *Proc. SPIE-Int. Soc. Opt. Eng.* **1997**, *3144*, 41−52. (c) Osaheni, J. A.; Jenekhe, S. A.; Perlstein, J. *J. Phys. Chem.* **1994**, *98*, 12727−12736. (d) Osaheni, J. A.; Jenekhe, S. A.; Perlstein, J. *Appl. Phys. Lett.* **1994**, *64*, 3112−3114. (e) Abkowitz, M. A.; Stolka, M.; Antoniadis, H.; Agrawal, A. K.; Jenekhe, S. A. *Solid State Commun.* **1992**, *83*, 937−941. (f) Antoniadis, H.; Abkowitz, M. A.; Osaheni, J. A.; Jenekhe, S. A.; Stolka, M. *Synth. Met.* **1993**, *60*, 149−157.

(6) Garnier, F. *Chem. Phys.* **1998**, *227*, 253−262.

(7) Berggren, M.; Inganas, O.; Gustafsson, G.; Rasmusson, J.; Andersson, M. R.; Hjertberg, T.; Wennerstrom, O. *Nature* **1994**, *372*, 444−446.

(8) (a) Jenekhe, S. A.; Zhang, X.; Chen, X. L.; Choong, V.-E.; Gao, Y.; Hsieh, B. R. *Chem. Mater.* **1997**, *9*, 409−412. (b) Zhang, X.; Jenekhe, S. A. *Mater. Res. Soc. Symp. Proc.* **1998**, *488*, 539−544. (c) Hamaguchi, M.; Yoshino, K. *Appl. Phys. Lett.* **1996**, *69*, 143−145. (d) Wang, Y. Z.; Gebler, D. D.; Fu, D. K.; Swager, T. M.; Epstein, A. J. *Appl. Phys. Lett.* **1997**, *70*, 3215−3217.

(9) (a) Jenekhe, S. A.; Osaheni, J. A. *Science* **1994**, *265*, 765−768. (b) Osaheni, J. A.; Jenekhe, S. A. *Macromolecules* **1994**, *27*, 739−742. (c) Gebler, D. D.; Wang, Y. Z.; Blatchford, J. W.; Jessen, S. W.; Fu, D.-K.; Swager, T. M.; MacDiarmid, A. G.; Epstein, A. J. *Appl. Phys. Lett.* **1997**, *70*, 1644−1646. (d) Gebler, D. D.; Wang, Y. Z.; Fu, D.-K.; Swager, T. M.; Epstein, A. J. *J. Chem. Phys.* **1998**, *108*, 7842−7848.

(10) (a) Yang, C.-J.; Jenekhe, S. A. *Supramol. Sci.* **1994**, *1*, 91−101. (b) Lee, J.-I.; Kang, I.-N.; Hwang, D.-H.; Shim, H.-K. *Chem. Mater.* **1996**, *8*, 1925−1929. (c) Tasch, S.; List, E. J. W.; Hochfilzer, C.; Leising, G.; Schlichting, P.; Rohr, U.; Geerts, Y.; Scherf, U.; Mullen, K. *Phys. Rev. B: Condens. Matter* **1997**, *56*, 4479−4483.

(11) (a) Fou, A. C.; Onitsuka, O.; Ferreira, M.; Rubner, M. F.; Hsieh, B. R. *J. Appl. Phys.* **1996**, *79*, 7501−7509. (b) Onitsuka, O.; Fou, A. C.; Ferreira, M.; Hsieh, B. R.; Rubner, M. F. *J. Appl. Phys.* **1996**, *80*, 4067−4071.

(12) (a) Strukelj, M.; Papadimitrakopoulos, F.; Miller, T. M.; Rothberg, L. J. *Science* **1995**, *267*, 1969−1972. (b) Li, X. C.; Grimsdale, A. C.; Cervini, R.; Holmes, A. B.; Moratti, S. C.; Yong, T. C.; Gruner, J.; Friend, R. H. In *Photonic and Optoelectronic Polymers*; Jenekhe, S. A., Wynne, K. J., Eds.; ACS Symp. Series Vol. 672; American Chemical Society: Washington, DC, 1997. (c) Greenham, N. C.; Moratt, S. C.; Bradley, D. D. C.; Friend, R. H.; Holmes, A. B. *Nature* **1993**, *365*, 628−630. (d) O'Brien, D.; Weaver, M. S.; Lidzey, D. G.; Bradley, D. D. C. *Appl. Phys. Lett.* **1996**, *69*, 881−883. (e) Yamamoto, T.; Sugiyama, K.; Kushida, T.; Inoue, T.; Kanbara, T. *J. Am. Chem. Soc.* **1996**, *118*, 3930−3937. (f) Cui, Y.; Zhang, X.; Jenekhe, S. A. *Macromolecules* **1999**, *32*, 3824−3826. (g) Dailey, S.; Halim, M.; Rebourt, E.; Horsburgh, L. E.; Samuel, I. D. W.; Monkman, A. P. *J. Phys.: Condens. Matter* **1998**, *10*, 5171−5178.

(13) (a) Chen, X. L.; Jenekhe, S. A. *Macromolecules* **1997**, *30*, 1728−1733. (b) Jenekhe, S. A.; de Paor, L. R.; Chen, X. L.; Tarkka, R. M. *Chem. Mater.* **1996**, *8*, 2401−2404.

(14) (a) Yu, G.; Nishino, H.; Heeger, A. J.; Chen, T.-A.; Rieke, R. D. *Synth. Met.* **1995**, *72*, 249−252. (b) Zhang, X.; Shetty, A. S.; Jenekhe, S. A. *Proc. SPIE-Int. Soc. Opt. Eng.* **1997**, *3148*, 89−101.

(15) (a) Chen, X. L.; Jenekhe, S. A. *Macromolecules* **1996**, *29*, 6189−6192. (b) Chen, X. L.; Jenekhe, S. A. *Appl. Phys. Lett.* **1997**, *70*, 487−489. (c) Wagaman, M. W.; Bellmann, E.; Grubbs, R. H. *Philos. Trans. R. Soc. London, Ser. A* **1997**, *355*, 727−734. (d) Chen, X. L.; Jenekhe, S. A. *Synth. Met.* **1997**, *85*, 1431−1434.

(16) (a) Antoniadis, H.; Abkowitz, M. A.; Hsieh, B. R. *Appl. Phys. Lett.* **1994**, *65*, 2030−2032. (b) Blom, P. W. M.; de Jong, M. J. M.; Vleggaar, J. J. M. *Appl. Phys. Lett.* **1996**, *68*, 3308−3310. (c) Lin, L. B.; Jenekhe, S. A.; Borsenberger, P. M. *J. Chem. Phys.* **1996**, *105*, 8490−8494. (d) Lin, L. B.; Jenekhe, S. A.; Borsenberger, P. M. *Appl. Phys. Lett.* **1996**, *69*, 3495−3497.

(17) (a) Leising, G.; Tasch, S.; Meghdadi, F.; Athouel, L.; Froyer, G.; Scherf, U. *Synth. Met.* **1996**, *81*, 185−189. (b) Leising, G.; Tasch, S.; Brandstatter, C.; Graupner, W.; Hampel, S.; List, E. J. W.; Meghdadi, F.; Zenz, C.; Schlichting, P.; Rohr, U.; Geerts, Y.; Scherf, U.; Mullen, K. *Synth. Met.* **1997**, *91*, 41−47.

(18) (a) Grice, A. W.; Bradley, D. D. C.; Bernius, M. T.; Inbasekaran, M.; Wu, W. W.; Woo, E. P. *Appl. Phys. Lett.* **1998**, *73*, 629−631. (b) Pei, Q.; Yang, Y. *J. Am. Chem. Soc.* **1996**, *118*, 7416−7417. (c) Lee, J. I.; Klaerner, G.; Miller, R. D. *Chem. Mater.* **1999**, *11*, 1083−1088.

(19) (a) Kugler, T.; Johansson, A.; Dalsegg, I.; Gelius, U.; Salaneck, W. R. *Synth. Met.* **1997**, *91*, 143−146. (b) *Handbook of Chemistry and Physics*, 68th ed.; Weast, R. C., Astle, M. J., Beyer, W. H., Eds.; CRC Press: Boca Raton, FL, 1987−1988; p E-89.

(20) Tang, C. W.; Van Slyke, S. A. *Appl. Phys. Lett.* **1987**, *51*, 913−915.

(21) (a) Salaneck, W. R.; Strafstrom, S.; Bredas, J.-L. *Conjugated Polymer Surfaces and Interfaces*; Cambridge University Press: Cambridge, 1996. (b) Kugler, T.; Logdlund, M.; Salaneck, W. R. *Acc. Chem. Res.* **1999**, *32*, 225−234. (c) Gao, Y. *Acc. Chem. Res.* **1999**, *32*, 247−255.

(22) (a) Antoniadis, H.; Abkowitz, M.; Hsieh, B. R.; Jenekhe, S. A.; Stolka, M. *Mater. Res. Soc. Symp. Proc.* **1994**, *328*, 377−382. (b) Parker, I. D. *J. Appl. Phys.* **1994**, *75*, 1656−1666.

(23) (a) Torres, W.; Fox, M. A. *Chem. Mater.* **1990**, *2*, 306−311. (b) Hillman, A. R.; Mallen, E. F. *J. Electroanal. Chem.* **1990**, *281*, 109−124.

(24) (a) Agrawal, A. K.; Jenekhe, S. A. *Chem. Mater.* **1996**, *8*, 579−589. (b) Alanko, A. K. MS Thesis, University of Rochester, Rochester, NY, 1995. (c) Osaheni, J. A.; Jenekhe, S. A. *Chem. Mater.* **1992**, *4*, 1282−1290. (d) Osaheni, J. A.; Jenekhe, S. A. *Chem. Mater.* **1995**, *7*, 672−682.

(25) (a) Tunney, S. E.; Suenaga, J.; Stille, J. K. *Macromolecules* **1987**, *20*, 258−264. (b) Wnek, G. E.; Wasserman, B.; Dresselhaus, M. S.; Tunney, S. E.; Stille, J. K. *J. Polym. Sci., Polym. Lett. Ed.* **1985**, *23*, 609−612. (c) Osaheni, J. A.; Jenekhe, S. A.; Burns, A.; Du, G.; Joo, J.; Wang, Z.; Epstein, A. J. *Macromolecules* **1992**, *25*, 5828−5835. (d) Long, V. C.; Washburn, S.; Chen, X. L.; Jenekhe, S. A. *J. Appl. Phys.* **1996**, *80*, 4202−4204.

(26) (a) Agrawal, A. K.; Jenekhe, S. A. *Macromolecules* **1993**, *26*, 895−905. (b) Agrawal, A. K.; Jenekhe, S. A. *Macromolecules* **1991**, *24*, 6806−6808. (c) Osaheni, J. A.; Jenekhe, S. A. *Macromolecules* **1993**, *26*, 4726−4728. (d) Agrawal, A. K.; Jenekhe, S. A. *Chem. Mater.* **1993**, *5*, 633−640.

(27) (a) Jenekhe, S. A.; Johnson, P. O.; Agrawal, A. K. *Macromolecules* **1989**, *22*, 3216−3222. (b) Jenekhe, S. A.; Johnson, P. O. *Macromolecules* **1990**, *23*, 4419−4429. (c) Yang, C. J.; Jenekhe, S. A. *Chem. Mater.* **1991**, *3*, 878−887.

(28) Greenham, N.; Friend, R. H.; Bradley, D. C. C. *Adv. Mater.* **1994**, *6*, 491.

(29) (a) Agrawal, A. K.; Jenekhe, S. A. *Chem. Mater.* **1992**, *4*, 95−104. (b) Gymer, R. W.; Friend, R. H.; Ahmed, H.; Burn, P. L.; Kraft, A. M.; Holmes, A. B. *Synth. Met.* **1993**, *55*−*57*, 3683.

(30) (a) Zhang, X.; Shetty, A. S.; Jenekhe, S. A. *Macromolecule* **1999**, *32*, 7422−7429. (b) Osaheni, J. A.; Jenekhe, S. A. *J. Am. Chem. Soc.* **1995**, *117*, 7389−7398.

(31) Wool, R. P. *Polymer Interfaces*; Hanser Publishers: Cincinnati, OH, 1995.

(32) (a) Jenekhe, S. A.; Schuldt, S. B. *Ind. Eng. Chem. Fundam.* **1984**, *23*, 432−436. (b) Jenekhe, S. A. *Ind. Eng. Chem. Fundam.* **1984**, *23*, 425−432.

(33) Ishii, H.; Sugiyama, K.; Ito, E.; Seki, K. *Adv. Mater.* **1999**, *11*, 605−625.

(34) (a) Eckhardt, H.; Shacklett, L. W.; Jen, K. Y.; Elsenbaumer, R. L. *J. Chem. Phys.* **1989**, *91*, 1303−1315. (b) Bredas, J. L.; Silbev, R.; Boudreaux, D. S.; Chance, R. R. *J. Am. Chem. Soc.* **1983**, *105*, 6555−6559. (c) Jandke, M.; Strohriegl, P.; Berleb, S.; Werner, E.; Brutting, W. *Macromolecules* **1998**, *31*, 6434−6443.

(35) Gutmann, F.; Lyons, L. E. *Organic Semiconductors*; John Wiley & Sons: New York, 1967.

(36) In the case of emission from both layers, $\phi_{EL} = \gamma^1\eta^1\phi_{PL}{}^1 + \gamma^2\eta^2\phi_{PL}{}^2$, where the superscripts 1 and 2 represent different polymer layers.

(37) (a) Do, L. M.; Han, E. M.; Niidome, Y.; Fujihira, M.; Kanno, T.; Yoshida, S.; Maeda, A.; Ikushima, A. J. *J. Appl. Phys.* **1994**, *76*, 5118−5121. (b) Fujuhira, M.; Do, L. M.; Koike, A.; Han, E. M. *Appl. Phys. Lett.* **1996**, *68*, 1787−1789. (c) McElvain, J.; Antoniadis, H.; Hueschen, M. R.; Miller, J. N.; Roitman, D. M.; Sheats, J. R. *J. Appl. Phys.* **1996**, *80*, 6002−6007.

(38) (a) Allen, J. W. *J. Lumin.* **1994**, *60*−*61*, 912−915. (b) Kittel, C. *Introduction to Solid State Physics*, 6th ed.; John Wiley: New York, 1986; Chapter 19.

(39) Deussen, M.; Scheidler, M.; Bassler, H. *Synth. Met.* **1995**, *73*, 123−129.

MA991913K